Computational Chemistry and Aeroassisted Orbital Transfer Vehicles

D.M. Cooper,* R.L. Jaffe,† and J.O. Arnold‡
NASA Ames Research Center, Moffett Field, California

An analysis of the radiative heating phenomena encountered during a typical aeroassisted orbital transfer vehicle (AOTV) trajectory was made to determine the potential impact of computational chemistry on AOTV design technology. Both equilibrium and nonequilibrium radiation mechanisms were considered. This analysis showed that computational chemistry can be used to predict 1) radiative intensity factors and spectroscopic data; 2) the excitation rates of both atoms and molecules, 3) high-temperature reaction rate constants for metathesis and charge exchange reactions, 4) particle ionization and neutralization rates and cross sections, and 5) spectral line widths.

Nomenclature

E = total energy
H = Hamiltonian operator
r = internuclear separation
T = temperature
ψ = wave function

Subscripts

el = electronic
g = gas
vib = vibrational

Introduction

THE majority of previous Earth-entry investigations[1-3] focused on problems encountered by blunt bodies passing through the Earth's atmosphere at velocities between 6 and 20 km/s. These Apollo-type vehicles had to survive severe radiative and convective heating as they decelerated through the Earth's atmosphere. Ablative heat shields were used to protect the vehicles and their occupants. The critical heat shield design requirements stimulated an immense amount of research on the flowfield properties surrounding these vehicles. An important part of this research was the determination of the chemical and radiative properties of the gases in the surrounding shock layer. While some of this reseach was theoretical, the large majority of the work to determine the shock-heated gas properties was experimental.

Recent interest[4,5] in aeroassisted orbital transfer vehicles (AOTV) is beginning to stimulate research in a previously neglected phase of Earth entry. Two types of vehicles are currently under consideration. The first is an orbital transfer vehicle (OTV) designed to work in conjunction with the Space Shuttle. Its mission is the transport of payloads between the low Shuttle orbits and higher orbits. Preliminary results indicate that substantial savings in fuel can be obtained by having the vehicle make a single pass through the upper atmosphere to decelerate before rendezvousing with the Shuttle. The second is an orbit-on-demand vehicle. This is a small maneuverable vehicle that will take off from the Earth, orbit for approximately one day, and return to the Earth, landing like an aircraft. Both vehicles are designed to be reusable.

In contrast to the Apollo-type entry vehicles, AOTV trajectories will be largely in the low-density regions of the Earth's atmosphere. This complicates the prediction of the flowfield properties. For much of the trajectory of the Apollo entry, the density was high enough for the flow to be in local thermodynamic equilibrium. Dissociation and ionization rates occurred with sufficient rapidity for the gas to reach equilibrium conditions within 1 mm behind the shock front. However, initial investigations[6] of typical AOTV trajectories indicate that the gas in the shock layer is not in chemical or thermodynamic equilibrium. As a consequence, nonequilibrium radiation may dominate both convective and equilibrium radiative heating.[6,7] The question of nonequilibrium radiation in a vehicle shock layer has been studied; however, there are several major uncertainties that preclude any realistic estimates of its contributions to AOTV. The importance of nonequilibrium radiation and its contribution to the total heating is one of several technological AOTV problems that must be addressed. Fortunately, we no longer have to rely almost exclusively on experimental techniques. With the advent of large-scale computers, computational chemistry techniques[8,9] have advanced to the stage where they may successfully be used to accurately predict the chemical and radiative properties of atoms and molecules. Furthermore, these techniques have also been developed to predict the reaction rates of atomic and molecular excitation, ionization, and chemical reactions.

The purpose of this paper is to examine the problems surrounding radiative (equilibrium and nonequilibrium) heating mechanisms for AOTV and to apply computational chemistry methods to those best suited for theoretical solutions. It should be noted at the onset that theoretical techniques will not replace experimental methods, but will complement them. The role and advantages of computational chemistry for AOTVs in general will be stressed in the following sections. Since the AOTV is in the conceptual stage and its actual trajectories are not yet precisely defined, we cannot completely evaluate that total impact of theoretical chemistry on the overall project.

Application to AOTV Technology

Computational chemistry uses solutions to the Schrodinger equation, $H\psi = E\psi$, to determine the properties of atoms and molecules. The techniques used to solve this equation are well

Received March 9, 1984; revision received June 4, 1984. This paper is declared a work of the U.S. Government and therefore is in the public domain.

*Leader, Solid-Phase Computational Chemistry Group.
†Leader, Gas-Phase Computational Chemistry Group.
‡Chief, Computational Chemistry and Aerothermodynamics Branch.

documented and will not be described here. The methods most commonly used to successfully predict the structure and properties of molecules are the self-consistent field (SCF) plus configurations interaction (CI) and the multiconfiguration self-consistent field (MCSCF) plus CI techniques. These methods are used in most of the applications that follow.

Potential Energy Curves and Intensity Factors

Behind the shock front formed on the AOTV, radiation will originate from a number of sources.[6] These include atomic lines from N and O, atomic continua from N, O, N^+, and O^+, and emission from electronically excited diatomic molecules such as N_2, N_2^+, O_2, and NO. Other species such as O_2^+ and NO^+ will be present, but will not contribute much radiation since their concentrations are expected to be very small. However, they are expected to play important roles in determining the N_2^+ and NO concentration. The oscillator strengths (or Einstein A coefficients) for atomic N and O, as well as the cross sections for continuum radiation from N and O, are reasonably well known. In addition, the radiation from diatomic molecules is expected to dominate the total radiative flux.

There are many spectroscopic transitions possible for N_2, N_2^+, O_2, and NO.[10] Some of these are well known such as the N_2^+ first negative system, the O_2 Schumann-Runge system, and the N_2 Lyman-Birge-Hopfield system. However, others are not well categorized. Furthermore, the absolute strength of many of the band systems, including those readily identifiable such as the N_2 systems are not known. Table 1 contains a list of the band systems that are expected to be strong radiators on the AOTV. An estimate of the accuracy of the electronic transition moment is also listed. As shown, the absolute intensities of some systems are uncertain by as much as a factor of three. These uncertainties can be reduced, as demonstrated below, by theoretical quantum chemical calculations.

The SCF+CI method has been used to accurately predict the potential energy curves and the absolute value of the electronic transition moment between the electronic states for several molecules.[11-15] Figure 1 is a comparison of the theoretical potential energy curves for several states with the existing experimental RKR curves of CO. The theoretical and experimental curves are in very good agreement. Spectroscopic constants, which were obtained for the theoretical curves from a least-square fit to an extended Morse curve, are also in good agreement with the experimental values.

The sum of the squares of the theoretical electronic transition moment (a parameter that controls the overall radiation intensity for transitions between electronic states of molecules) for the CO fourth positive system is compared with the experimental data[13] in Fig. 2. For this system, the theoretical transition moment data support the experimental data that show a strong dependence on internuclear separation (or wavelength). The calculated values of the electronic transition moment for the NO beta and delta systems are compared with the existing experimental data[15] in Figs. 3 and 4, respectively.

For the beta system, the theory is in excellent agreement with the measurements of Hassen and Nicholls,[16] Farmer et al.,[17] and Bethke[18] (for $r>2.28$ Bohr). The measurements of Antropov et al.[19] and Keck et al.[20] appear to be much too large. For $r<2.28$ Bohr, the experimental data of Bethke vary by an order of magnitude. The reason for this variation is clarified by examining the theoretical potential energy curves for NO shown in Fig. 5. As illustrated in the figure, the potential energy curves for the $B\,^2\Pi$ and $C\,^2\Pi$ electronic states have an avoided crossing near 2.22 Bohr. This avoided crossing undoubtedly accounts for the large difference in magnitude between the $r=2.204$ and 2.228 Bohr measurements of Bethke. Consequently, these two measurements are probably neither meaningful nor valid for comparison with the other results shown in Fig. 3. Without the results of the

Table 1 Uncertainties in the electronic transition moments for molecular band systems

	Band system	Uncertainty factor
N_2	Lyman-Birge-Hopfield	3.0
N_2	Birge-Hopfield	3.0
N_2^+	Meinel	2.5
N_2	First positive	2.5
N_2	Second positive	2.0
N_2^+	First negative	2.0
NO	Gamma	1.8
O_2	Schumann-Runge	1.4
NO	Beta	1.2
NO	Delta	1.2

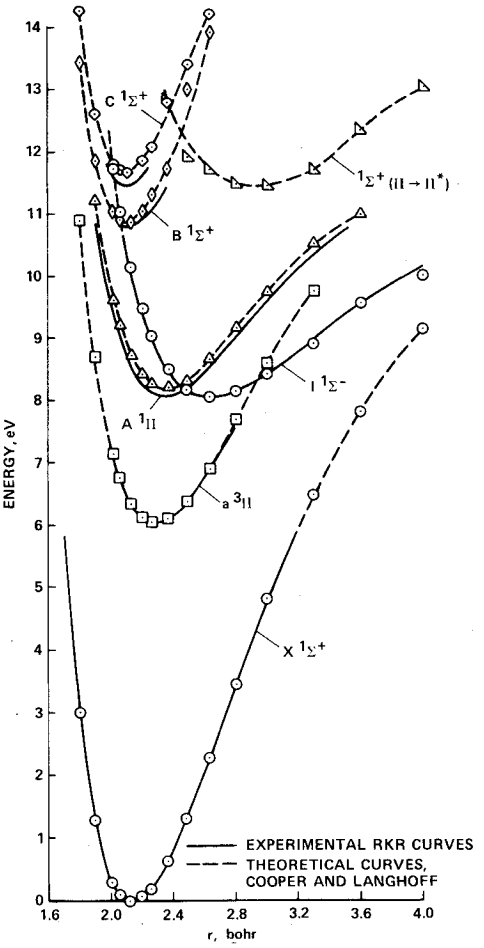

Fig. 1 Comparison of the theoretical potential energy curves (dashed) with the existing experimental RKR curves (solid) of CO.

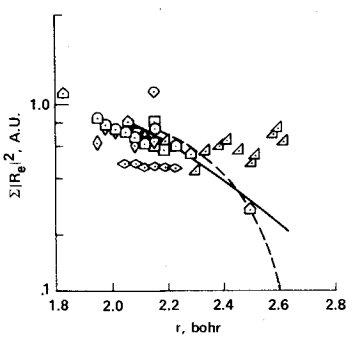

Fig. 2 Sum of the squares of the electronic transition moment for the CO fourth positive system, (solid curve repesents theoretical calculations, dashed curve and the symbols represent various experimental results).

theoretical calculations shown in Figs. 3 and 5, it would be almost impossible to obtain an accurate electronic transition moment variation for the NO beta system.

A similar statement could be made regarding the NO delta system in Fig. 4. According to Bethke, his measurements of the (0,0 and 1,0) vibrational levels ($r = 2.096$ and 2.149 Bohr, respectively) contain contributions from the NO beta system. This may account for the differences in Fig. 4 between the theoretical calcuations and his measurements at those points. A small extrapolation of the theory in Fig. 4 to large internuclear separations gives very good agreement with Bethke's only other data (the 2,0 vibrational band). The experimental data of Callear and Pilling,[21] which are almost a factor of three greater than the theory appear too large.

The results for CO and NO are typical of the accuracy and impact that computational chemistry can have in determining the absolute strength of molecular band systems. The absolute strengths or intensity factors for all of the diatomic molecules present in the shock-heated gas can and should be determined to reduce the uncertainties in the AOTV radiation model. It should be noted that the variation of the electronic transitions moment with internuclear separation must be known to accurately predict absolute emission intensities or photoabsorption cross sections. These variations are very difficult to obtain experimentally. There are many experimental techniques that use emission, absorption, or lifetime measurements to obtain electronic transition moments. However, the final results of each of these techniques are directly dependent on some combination of assumptions, approximations, or existing spectroscopic data. Any significant error in any one of these can render the results completely invalid. Alternatively, the variation of the electronic transitions moment can be accurately predicted theoretically (Figs. 2-4).

Excitation Rates

Initial calculations[6,7] of the heating rates for typical AOTV trajectories predict that nonequilibrium radiation will dominate the heating flux. This condition is primarily due to the extended flight time in the low-density regime of the Earth's atmosphere. The modeling of the nonequilibrium radiation requires a knowledge of the excitation rates for populating the emitting states of both atoms and molecules. The collisional processes that produce the energy level populations are extremely complex and include electron-atom, electron-molecule, ion-molecule, atom-atom, and

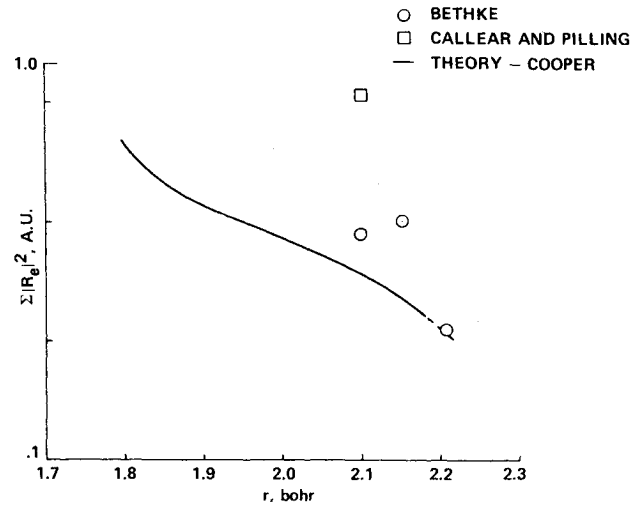

Fig. 4 Sum of the squares of the electronic transition moment for the NO delta system.

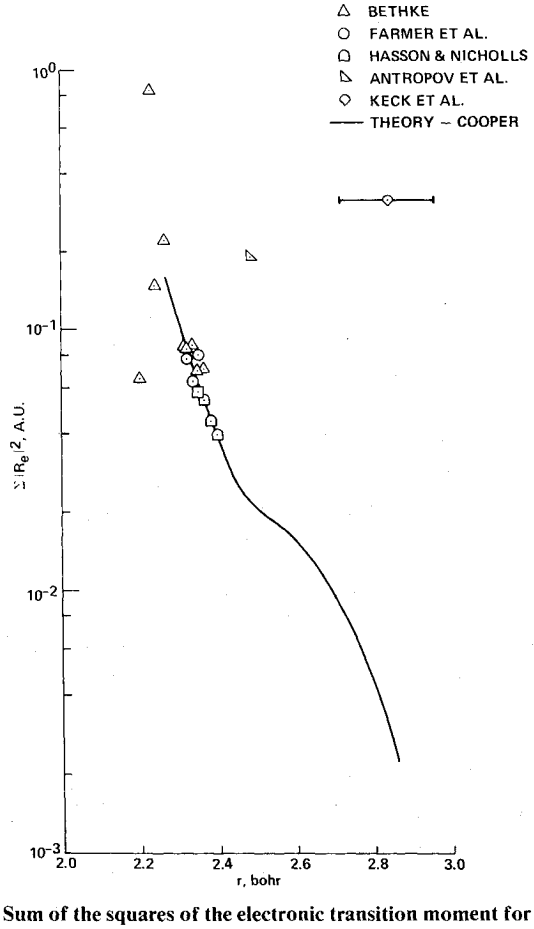

Fig. 3 Sum of the squares of the electronic transition moment for the NO beta system.

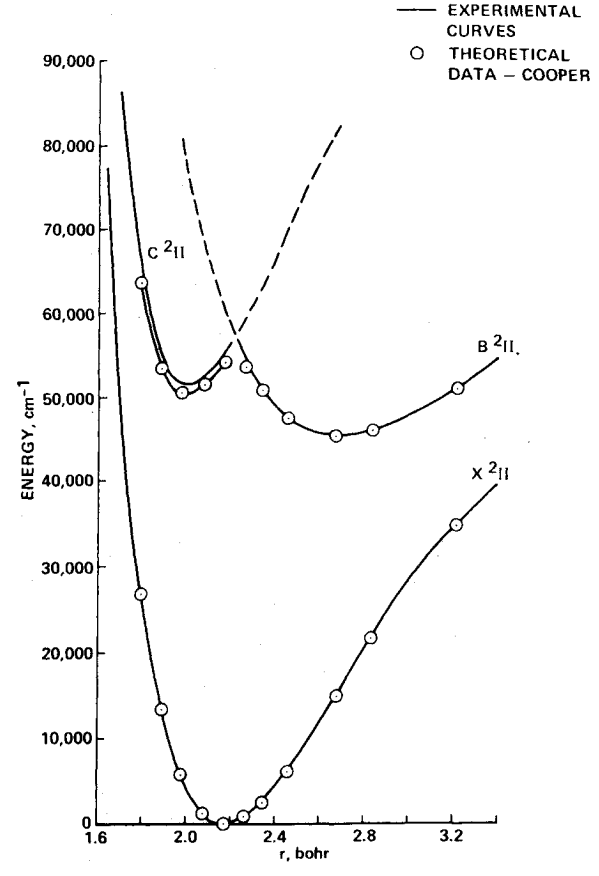

Fig. 5 Comparison of theoretical potential curves for the $X^2\Pi$, B $^2\Pi$, and C $^2\Pi$ electronic states of NO with the experimental Klein-Dunham curves.

atom-molecule collisions.[22] For N and O atoms, the excitation rates can be calculated to a fair degree of accuracy.[23] However, for molecules, the excitation rates cannot presently be accurately predicted. Further theoretical development is needed in order to accurately determine these molecular excitation rates. In addition, all of the low-lying electronic states of the molecules under consideration must be well known. It should be noted that one of the main contributions of computational chemistry is its ability to correctly define and sort excited states of molecules. Experimentally, this process is very complicated and difficult, especially for large molecules, and often leads to ambiguous results. By carefully choosing the proper basis set, however, the entire manifold of excited states can be easily determined theoretically.

As demonstrated above (Figs. 1 and 5), the current computational chemistry methods provide accurate predictions of both ground- and excited-state potential energy curves. The theoretical results accurately predict the shape of the potential energy curves, electronic term energies (the vertical separation of the curves on Figs. 1 and 5), and dissociation energies. Table 2 is a comparison of the theoretical and experimental values of the dissociation energies for several molecules. The success of the theory is obvious.

Since the population of excited molecular electronic states and the excitation rates of these states may be affected by predissociation[24] and inverse predissociation,[25] the impact of these processes must be evaluated. These phenomena are well known for the O_2 Schumann-Runge system,[24-25] but they are important for other molecules as well. For example, there is evidence for N_2 that the emitting state of the first positive system, $B\,^3\Pi_g$, is predissociated by the repulsive $^5\Sigma_g^+$ state. Figure 6 is a plot of the potential energy curves for N_2.[26] The shape and position of many of these curves are approximate. Note that the $^5\Sigma_g^+$ state crosses the $B\,^3\Pi_g$ state; consequently, there is a finite probability that a radiationless transition will take place from the $B\,^3\Pi_g$ state to the $^5\Sigma_g^+$ state and, thus, lower the energy required for dissociation from the $N(^4S) + N(^2D)$ limit to the $N(^4S) + N(^4S)$ limit.

It is also possible that the $N_2 B\,^3\Pi_g$ state could be populated directly by inverse predissociation during collisions of two ground-state N atoms. The impact of these processes on the excitation rate is controlled by two factors: 1) the location of the crossing point between the $B\,^3\Pi_g$ and the $^5\Sigma_g^+$ states (the crossing point on Fig. 6 is only approximate) and 2) the strength of the coupling of the two states. The exact location of the crossing and the spin-orbit coupling matrix elements that govern the strength of the predissociation can also be accurately calculated. A complete theoretical investigation of the electronic structure of N_2, including predissociation effects, would help clarify the excitation rates and thus reduce the uncertainties in the nonequilibrium model. Calculations of this type have been performed on OH and the results are in good agreement with the experimental data.[27]

Table 2 Comparison of theoretical and experimental dissociation energies

	Dissociation energy, eV		
Molecule	Theoretical	Experimental	
OH	4.62	±0.01	4.63
CN	7.89	±0.13	8.02
SiO	8.20	±0.12	8.25
ClO	2.75	±0.001	2.803
C_2	6.17	±0.20	6.25
CO	10.86	±0.13	11.23
LiH	2.48	±0.02	2.52

Rate Constants for Metathesis and Charge Exchange Reactions

The chemistry leading to the expected distribution of emitting molecules is extremely complex even though only 10 atomic and diatomic species are involved (N, O, N_2, O_2, NO, and their corresponding positive ions). Processes resulting from electron-atom and molecule, ion-neutral, atom-atom, and atom-molecule collisions all must be considered to model the atomic, N_2^+, and NO production rates.[28] In the nonequilibrium regime, anticipated for typical AOTV trajectories, $T_g \simeq 20{,}000$ K and $T_{vib} = T_{el} = 10{,}000$ K. In order to model the kinetics, very-high-temperature rate constant data are needed; however, most of the important processes have been studied only at temperatures encountered in combustion or ionospheric chemistry, i.e., less than 5000 K. It is extremely risky to extrapolate even accurate 300-5000 K rate constant data to 20,000 K as the entire nature of the reaction could change over such a large temperture range.[29,30] In addition, the lack of complete thermal equilibrium ($T_{vib} \neq T_g$) implies that thermal rate constants are inappropriate for the problem. Few guidelines exist for extracting the necessary kinetics data from existing measurements.

Again, theoretical chemistry can be called upon to provide some of the needed data. Rate constants for atom-diatom or diatom-diatom reactions generally can be computed from first principles, provided accurate potential energy surfaces exist for the three or four atom systems.[31-34] Potential energy surfaces (PES) can be computed using MCSCF + CI methods in an analogous manner to the prediction of diatomic molecule potential energy curves. The task is more difficult, however, as additional degrees of freedom must be considered and the critical points on the PES (energy barriers or transition states) correspond to polyatomic geometries with two or more partially formed chemical bonds. The former com-

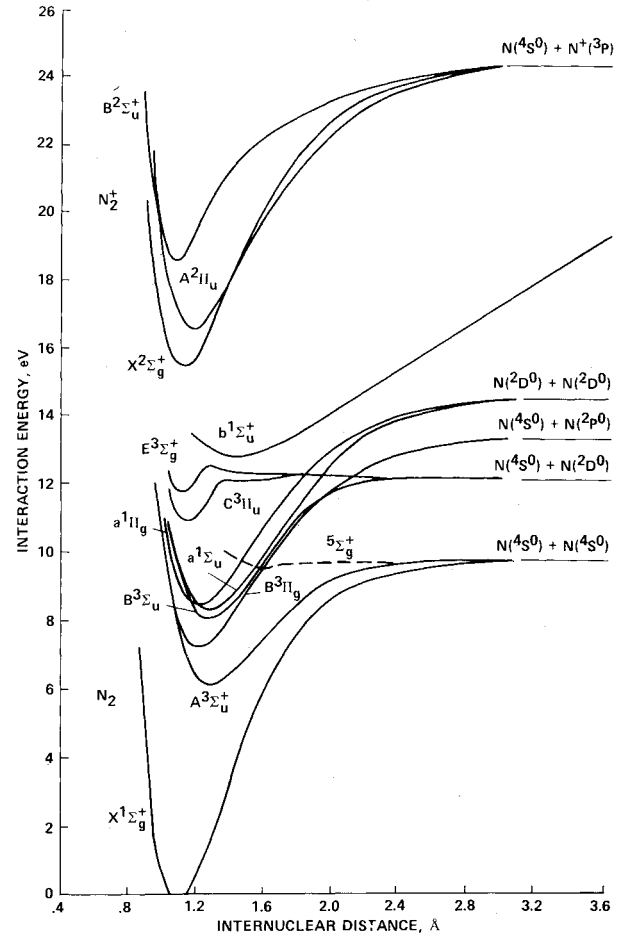

Fig. 6 Potential energy curves for selected electronic states of N_2 and N_2^+.

plication means the energy must be calculated for many geometries and the latter requirement means that each energy calculation must include many more terms than typically employed for diatomics. Due to the incumbent difficulties, full-scale accurate PES calculations have only been reported for simple reacting systems such as $H_2 + H \rightarrow H + H_2$ (Ref. 35) and $H_2 + F \rightarrow H + HF$ (Ref. 36). However, transition state energies and structures have been predicted for many more complicated chemical reactions.

Once the PES has been determined, the collisional processes can be simulated over the entire temperature range of interest using classical mechanics.[31] The trajectories of individual reactive (or inelastic) collisions are computed by solving the classical equations of motion using statistically chosen initial conditions and the PES as input. Based on Monte Carlo sampling techniques, rate constants can be predicted from the results of a few thousand trajectories. Nonequilibrium effects can be studied by selecting the diatomic vibrational energies and the collision energies from different distributions. Classical trajectory calculations have been carried out for numerous atom-diatom and diatom-diatom reactions. Most of the studies have been semiquantitative in nature since accurate PESs were not available. However, for the $H_2 + H$ (Ref. 37) and $H_2 + F$ (Ref. 38) exchange reactions, the results are in excellent agreement with the experiment and with rigorous quantum mechanical scattering calculations.

It would take the dedication of considerable human and computer resources to calculate the rate-constant data needed for the AOTV conditions. However, given a critical need for these data, potential energy surfaces for three atom-systems like NNO and NOO can be computed and high-temperature rate constants can be predicted for the corresponding $N_2 + O \rightarrow N + NO$ and $O_2 + N \rightarrow O + NO$ metathesis reactions (to supplement the existing low-temperature data[39]).

The calculation of rate constants for ion-neutral reactions is even more complicated since competing metathesis and charge-transfer pathways exist. At least two potential energy surfaces are required to describe the collision.[40] These PESs exhibit regions of avoided crossing where the charge transfer can occur.[41] A trajectory is actually permitted to "hop" from one surface to another while traversing the avoided-crossing regions. The product of the surface-hopping probabilities for all the times the trajectory passes through the avoided-crossing region determines the overall probability of charge transfer. The probability of reaction (i.e., atom transfer) is governed by the topography of the PES and is only loosely coupled to the charge-transfer probability. Competing cross sections for metathesis and charge exchange have been successfully computed for $H_2 + H^+$ (Ref. 42) and $H_2 + R^+$ (Ref. 43), where R is a rare-gas atom, using this "surface hopping" trajectory method.

For the AOTV problem, one such ion-neutral reaction system that might be studied is NOO^+. Six different elementary reactions are possible:

$$O_2 + N^+ \rightarrow O_2^+ + N + 2.5\text{eV} \quad (1)$$

$$O_2 + N^+ \rightarrow NO^+ + O + 6.7\text{eV} \quad (2)$$

$$O_2 + N^+ \rightarrow NO + O^+ + 2.3\text{eV} \quad (3)$$

$$O_2^+ + N \rightarrow NO^+ + O + 4.2\text{eV} \quad (4)$$

$$NO + O^+ \rightarrow O_2^+ + N + 0.2\text{eV} \quad (5)$$

$$NO + O^+ \rightarrow NO^+ + O + 4.4\text{eV} \quad (6)$$

Reaction (2), (4), and (5) are atom transfers, (1) and (6) are charge exchange processes, and (3) involves both atom transfer and charge exchange. The low-lying diatomic neutral and ion potential curves are shown in Fig. 7. The curves have been shifted to a common reference energy appropriate for $N + O + O^+$, so the relative reactant and product channels may be observed. It is important to note that the problem is further complicated by the presence of electronically excited atoms and diatomic ions. Depending on the processes to be studied, as many as five different PESs could be needed to fully describe the kinetics.

Limited experimental data exist for the NOO^+ system; all reactions[43-45] except (3) and (5) have been observed in low-temperature experiments. In general, the rate constants for these ion-neutral reactions exhibit a slight negative temperature dependence between 300 and 700 K and are independent of temperature between 700 and 1500 K. However, qualitative theories of ion-molecule kinetics predict the rate constants to increase at higher temperatures.[46] The charge transfer process (6) has been studied as a function of ion energy (T_g). The rate constant increases rapidly with temperature, so this process would be more than 100 times faster under AOTV conditions than at room temperature. Similar increases in rate constants are possible for the other steps as well. Thus, considerable uncertainties exist in the extrapolation of low-temperture kinetic data to 20,000 K. If sensitivity studies of the AOTV nonequilibrium model demonstrate the importance of these ion-neutral processes, selected rate constants could be predicted using theoretical chemistry methods.

Ionization and Neutralization Phenomena

One of the significant features of the nonequilibrium model is the importance of ionization and electron-ion recombination processes.[6,28] These include the associative ionization (AI) of NO: $N + O \rightarrow NO^+ + e^-$, which is likely to be the initial source of electrons, and the dissociative recombination (DR) of N_2^+, O_2^+, and NO: e.g., $O_2^+ + e^- \rightarrow O + O$. These processes have been studied extensively at low temperatures (300-3000 K) due to their importance in the ionosphere.[47] However, nothing is known about AI and DR rates at the higher temperatures expected for AOTV. It is well established that, for $T_{vib} = T_{el} = 10{,}000$ K, many more channels for recombination will open up and the rate constants may become quite large. In contrast to some of the parameters discussed above, these rate constants can be accurately measured at all temperatures using experimental techniques. However, as described below, the theoretical work is not only capable of producing results, but it can also guide the experimental research and help interpret the results by providing a clear understanding of the potential energy curves and the curve crossings.

Computational techniques have been developed and proven for studying dissociative recombination.[48] These techniques are equally applicable to the study of associative ionization since AI is simply the reverse process of DR.[49] The calculation of DR rate constants is accomplished in two stages. First, the diatomic ion potential energy curve and the Rydberg and repulsive valence electronic state potential curves of the neutral are computed. Often a qualitative understanding of the DR mechanism can be obtained by inspection of these curves. Direct DR involves a transition from the ion to a repulsive neutral potential energy curve. The two curves must cross near an outer vibrational turning point of the ion for rapid dissociation to occur from that vibrational level. If the curves cross at an inner turning point, the unstable neutral species will undergo autoionization before dissociating.

In addition, there are electronic selection rules to determine which repulsive electronic states will interact strongly with the ion. On the other hand, indirect DR involves a transition from the ion to a Rydberg state of the neutral. This metastable species is subsequently predissociated by a repulsive valence state. The second stage involves computing the electronic

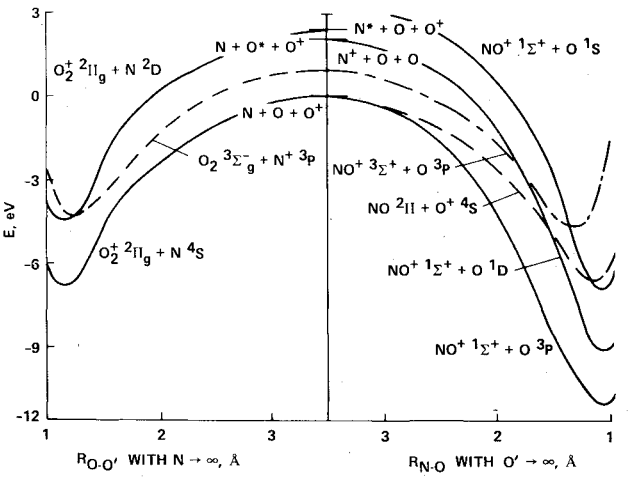

Fig. 7 Schematic representation of diatomic neutral and ion potential curves relevant to the NOO^+ reaction system. The curves have been placed on a common triatomic energy scale by addition of the appropriate atom energy. Energies are given relative to the lowest $N+O+O^+$ level. Solid curves are for diatomic ion plus ground or excited atoms. Dashed curves are for neutral diatomic plus atomic ion and the dot-dashed curve is for electronically excited diatomic ion plus atom.

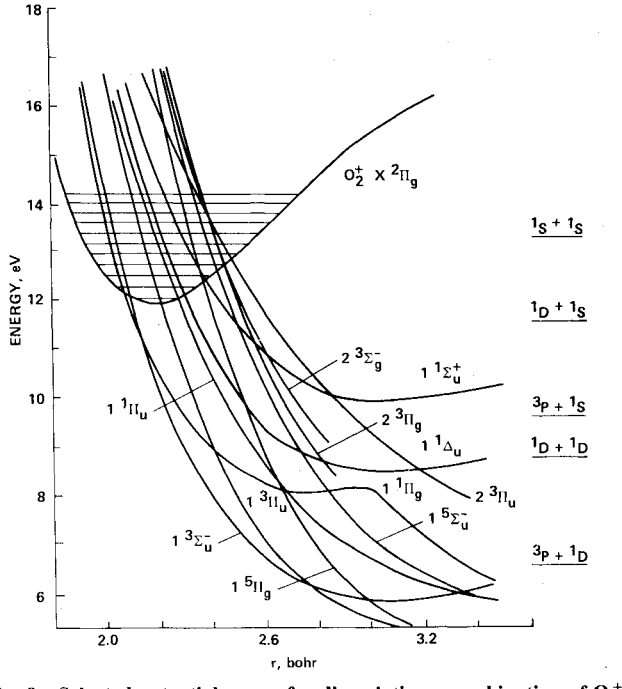

Fig. 8 Selected potential curves for dissociative recombination of O_2^+ (all O_2 repulsive valence curves crossing below $v=4$ are shown along with their dissociation products; the asymptotic O + O energy levels are also shown). Data taken from Ref. 48.

coupling matrix element between the ion plus free electron and the neutral diatomic. The DR cross section (or stength) of the interaction is proportional to the square of this matrix element. The overall DR rate constant is obtained by summing the overall probable transitions with the appropriate vibrational populations for the ion as given by T_{vib}.

Guberman has computed dissociative recombination cross sections for O_2^+ at ionospheric temperatures.[48] He has considered all 62 valence states of O_2 which can be formed from ^3P, ^1D, and ^1S oxygen atoms. Of these, 29 satisfy the electronic selection rules, but only the 9 which cross the $O_2^+ X\ {}^2\Pi_g$ potential curve between the R_e (1.12A) and the outer vibrational turning point for $V=4$ (1.35A) can contribute to the DR cross sections from low O_2^+ vibrational levels. The O_2^+ and selected neutral potential energy curves are shown in Fig. 8. The actual dissociation rates and branching ratios for forming O ^3P, ^1D, or ^1S depend on the magnitudes of the nine electronic coupling matrix elements. For high vibrational temperatures, the contributions of many more valence states to the overall DR rate will have to be determined.

Spectral Line Broadening

When the dimensions of the flowfield are large and self-absorption of radiation becomes important, the spectral line widths of both atoms and molecules are needed for radiative transport calculations to determine the total radiative heating flux. This may be the case for the AOTVs. The possible broadening mechanisms include natural broadening, Doppler broadening, and Stark or pressure broadening. Estimates[6] of the thermodynamic conditions in the shock layer for a typical AOTV trajectory indicate that pressure broadening will dominate the above mechanisms. Pressure broadening results from the collision of a radiating particle with the other particles in the gas. The collisions may involve atomic and diatomic neutral particles, ions, and electrons. Since a radiating particle is perturbed more strongly by a charged particle than a neutral one, the effect of neutral particles may be neglected if sufficient ionization takes place. Furthermore, pressure broadening is density dependent. These facts further demonstrate the need to know the thermodynamic conditions and composition of the gas in the shock layer. As shown above, it is reasonable to assume that the following species may play an important role as either a radiator or a perturber in the gaseous AOTV shock layer: N, O, N^+, O^+, e^-, N_2, N_2^+, O_2, O_2^+, NO, and NO^+.

Quantum mechanical treatments of the general theory of pressure broadening for atoms and ionized atoms have been given by Baranger[50] and Griem.[23] Griem lists pressure broadening parameters for many lines of both neutral and single ionized N and O atoms. Wilson and Nicolet[51] have expanded that list to include most of the important atomic lines of N, O, N^+, and O^+. Consequently, most of the line width parameters for atomic lines occuring in the AOTV shock layers are reasonably well known.

The techniques for calculating the broadening parameters and shapes of molecular rotational lines are similar to those for atoms. Anderson[52] and Tsao and Curnutte[53] have developed general quantum mechanical theories for rotational line broadening. By making various approximations and simplifying assumptions, several researchers[54-59] have successfully applied the theory to calculate the pressure broadening of specific molecules. Thomas and Nordstom[59] have given perhaps the most detailed and descriptive application of the molecular line broadening theory. It should be noted that, while the computational procedures for calculating the broadening of atomic and molecular lines are similar, the complexity of the molecular broadening problem is immense. For atoms, the energy levels must be known to calculate the line widths. These are accurately known for many atoms and ions and certainly well known for N, O. N^+, and O^+, the atomic particles of interest for AOTV entry. For molecules, however, the additional mechanisms of vibration and rotation require that the entire potential energy surface be accurately known. The potential energy curves for molecules are not frequently well known. The potential energy curves for N_2, O_2, NO, and their ions all need refinement in order to predict reasonable pressure broadening line widths for these species. The complexity of the molecular line broadening problem is also enhanced by the fact that dipole-dipole interactions, dipole-quadropole interactions, exchange forces, induction forces, and dispersion forces must be considered. Furthermore, the level of effort required to calculate molecular line widths is magnified since the widths of each of the radiating particles interacting with each of the perturbers must be determined.

Summary

An analysis of the radiative (equilibrium and nonequilibrium) heating phenomena encountered during a typical AOTV trajectory was made to determine the potential contribution of theoretical chemistry to the problems impacting AOTV. This investigation revealed several areas in which computational chemistry could contribute to the technology base required for AOTV design. Specifically, computational chemistry techniques are ideally suited to determine molecular potential energy curves and surfaces, transitions between energy states, and the intensity factors regulating these transitions. These factors are needed to predict the absolute levels of radiation in the shock layer formed on AOTVs. Computational chemistry methods can be used to predict: 1) the excitation rates for populating the emitting states of both atoms and molecules; 2) the high-temperature reaction rate constants for metathesis and charge exchange reactions; and 3) particle ionization and neutralization rates and cross sections. These rates are required to accurately model and predict the nonequilibrium radiation that is expected to dominate the heating flux during AOTV entry. The spectral line widths required to predict the total heating may also be determined using theoretical chemistry methods. Clearly, comptutional chemistry techniques can be used to provide solutions to many of the AOTV design problems. Some of the theoretical calculations (i.e., reaction rate and line broadening determinations) require considerable manpower and computer resources. Consequently, sensitivity studies to determine the importance of each of the transitions, reaction rates, etc., must be a prerequisite to the theoretical chemistry calculations.

References

[1]Bevans, J.T. (ed.), *AIAA Progress in Astronautics and Aeronautics: Thermal Design Principles of Spacecraft and Entry Bodies,* Vol. 21, Academic Press, New York, 1969.

[2]Bevans, J.T. (ed.), *AIAA Progress in Astronautics and Aeronautics: Thermophysics: Applications to Thermal Design of Spacecraft,* Vol. 23, Academic Press, New York, 1970.

[3]Heller, G.D. (ed.), *AIAA Progress in Astronautics and Aeronautics: Thermophysics and Temperature Control of Spacecraft and Entry Vehicles,* Vol. 18, Academic Press, New York, 1966.

[4]Walberg, G.D., "A Review of Aeroassisted Orbit Transfer," AIAA Paper 82-1378, Aug. 1982.

[5]Howe, J.T., "Introductory Aerothermodynamics of Advanced Space Transportation Systems," Journal of Spacecraft and Rockets, Vol. 22, Jan.-Feb. 1985, pp. 19-26.

[6]Park, C., "Radiation Enhancement by Nonequilibrium in Earth's Atmosphere," *Journal of Spacecraft and Rockets,* Vol. 22, Jan.-Feb. 1985, pp. 27-36.

[7]Menees, G.P., "Trajectory Analysis of Radiative Heating for Planetary Missions with Aerobraking of Spacecraft," *Journal of Spacecraft and Rockets,* Vol. 22, Jan.-Feb. 1985, pp. 37-45.

[8]Schaefer, H.F. III (ed.)., *Methods of Electronic Structure Theory,* Plenum Press, New York, 1975.

[9]Schaefer, H.F. III (ed.), *Applications to Electronic Structure Theory,* Plenum Press, New York, 1977.

[10]Suchard, S.N. (ed.), *Spectroscopic Data,* Vol. 1 and 2, Plenum Press, New York, 1975.

[11]Arnold, J.O., Whiting, E.E., and Langhoff, S.R., "MC-SCF+CI Wavefunctions and Properties of the $X\ ^2\Pi$ and $A^2\Sigma^+$ States of ClO," *Journal of Chemical Physics,* Vol. 66, 1977, p. 4459.

[12]Langhoff, S.R. and Arnold, J.O., "Theoretical Study of the $X^1\Sigma^+$, $A\ ^1\Pi$, $C^1\Sigma^-$, and $E^1\Sigma^+$ States of the SiO Molecule," *Journal of Chemical Physics,* Vol. 70, 1979, p. 852.

[13]Cooper, D.M. and Langhoff, S.R., "A Theoretical Study of Selected Singlet and Triplet States of the CO Molecule," *Journal of Chemical Physics,* 1981, p. 1200.

[14]Cooper, D.M., "Theoretical Electronic Transition Moments for the Ballik-Ramsay, Fox-Herzberg, and Swan Systems of C_2," *Journal of Quantitative Spectroscopy & Radiative Transfer,* Vol. 26, 1981, p. 113.

[15]Cooper, D.M., "Theoretical Study of IR Band Intensities and Electronic Transition Moments for the β and δ Systems of NO," *Journal of Quantitative Spectroscopy & Radiative Transfer,* Vol. 27, 1982, p. 459.

[16]Hasson, V. and Nicholls, R.W., "Application of Dispersion Techniques to Molecular Band Intensity Measurements. I. Oscillatory Strength of the (0,0) Band of NO-$\beta(B^2\Pi - X^2\Pi)$ System," *Journal of Physics B: Atomic and Molecular Physics,* Vol. 4, 1971, p. 1769.

[17]Farmer, A.J.D., Hasson, V., and Nicholls, R.W., "Absolute Oscillator Strength Measurements of the $(V''=0, v'=3)$ Bands of the $(A^2\Sigma - X^2\Pi)$ γ-System of Nitric Oxide," *Journal of Quantitative Spectroscopy & Radiative Transfer,* Vol. 12, 1972, p. 627.

[18]Bethke, G.W., "Oscillator Strengths in the Far Ultraviolet. I. Nitric Oxide," *Journal of Chemical Physics,* Vol. 31, 1959, p. 662.

[19]Antropov, E.T., Dronov, A.P., Sobolev, N.N., and Cheremisinov, V.P., "Experimental Determination of the Matrix Element of the Electron Transition in γ and β Systems of the NO Molecule," *Soviet Physics—Doklady,* Vol. 8, 1964, p. 1073.

[20]Keck, J.C., Camm, J.C., Kivel, B., and Wentink, T., "Radiation from Hot Air. Part II. Shock Tube Study of Absolute Intensities," *Annals of Physics,* Vol. 7, 1959, p. 1.

[21]Callear, A.B. and Pilling, M.J., "Fluorescence of Nitric Oxide," *Transactions of the Faraday Society,* Vol. 66, 1959, p. 1886.

[22]Flagan, R.C. and Appleton, J.P., "Excitation Mechanisms of the Nitrogen First-Positive and First-Negative Radiation at High Temperature," *Journal of Chemical Physics,* Vol. 56, 1972, p. 1163.

[23]Griem, H.R., *Plasma Spectroscopy,* McGraw-Hill Book Co., New York, 1964.

[24]Julienne, P.S. and Krauss, M., "Predissociation of the Schumann-Runge Bands of O_2," *Journal of Molecular Spectroscopy,* Vol. 56, 1975, p. 270.

[25]Myers, B.F. and Bartle, E.R., "Shock-Tube Study of the Radiative Combination of Oxygen Atoms by Inverse Predissociation," *Journal of Chemical Physics,* Vol. 48, 1968, p. 3935.

[26]Gilmore, F.R., "Potential Energy Curves for N_2 NO, O_2, and Corresponding Ions," *Journal of Quantitative Spectroscopy & Radiative Transfer,* Vol. 5, 1965, p. 369.

[27]Langhoff, S.R., Sink, M.L., Pritchard, R.H., and Kern, C.W., "Theoretical Study of the Spin-Orbit Coupling in the $X\ ^2\Pi$ State of OH," *Journal of Molecular Spectroscopy,* Vol. 96, 1982, p. 200.

[28]Park, C. and Menees, G.P., "Odd Nitrogen Production by Meteoroids," *Journal of Geophysical Research,* Vol. 83, 1978, p. 4029.

[29]Blais, N.C., Truhlar, D.G., and Garrett, B.C., "Dynamical Calculation of the Temperature Dependence of the Activation Energy for a Chemical Reaction from 444 to 2400 K," *Journal of Physical Chemistry,* Vol. 85, 1981, p. 1094.

[30]Eyring, H. and Leu, A.L., "Fall-Off from Extrapolated Values of All Chemical Reactions at Very High Temperatures," *Proceedings of the National Academy of Sciences, USA,* Vol. 72, 1975, p. 1717.

[31]Bunker, D.L., "Classical Trajectory Methods," *Methods in Comptutational Physics,* Vol. 10, 1971, p. 287.

[32]Jaffe, R.L. and Anderson, J.B., "Classical Trajectory Analysis of the Reaction $F+H \rightarrow HF+H$," *Journal of Chemical Physics,* Vol. 54, 1971, p. 2224.

[33]Jaffe, R.L., Henry, J.M., and Anderson, J.B., "Molecular Dynamics of the Hydrogen Iodide and Hydrogen-Iodine Exchange Reactions," *Journal of the American Chemical Society,* Vol. 98, 1976, p. 1140.

[34]Jaffe, R.L., "Calculated Rate Constants for the Reaction $ClO+O \rightarrow Cl+O$ between 220 and 1000 K," *Chemical Physics,* Vol. 40, 1979, p. 185.

[35]Siegbahn, P. and Liu, B., "An Accurate Three-Dimensional Potential Energy Surface for H_3," *Journal of Chemical Physics,* Vol. 68, 1978, p. 2457.

[36]Bender, C.F., Garrison, R.J., and Schaefer, H.F., "A Critical Test of 8 Semiempirical FH_2 Potential Energy Surfaces: The Barrier Height for $H+FH \rightarrow HF+H$," *Journal of Chemical Physics,* Vol. 62, 1975, p. 1188.

[37]Truhlar, D.G. and Horowitz, C.J., "Functional Representation of Liu and Siegbahn's Accurate *ab initio* Potential Energy calculations for $H+H_2$," *Journal of Chemical Physics,* Vol. 68, 1978, p. 2466.

[38]Polamyi, J.C. and Schreiber, J.L., "The Reaction $F+H_2 \rightarrow HF+H$: A Case Study in Reaction Dynamics," *Discussions of the Faraday Society,* Vol. 62, 1976.

[39]Hanson, R.K., Flower, L., and Kruger, C.H., "Determination of the Rate Constant for the Reaction $O+NO \rightarrow N+O_2$," *Combustion Science and Technology,* Vol. 9, 1974, p. 79.

[40]Kaufman, J.J., "Theoretical Considerations of Potential Energy Surfaces for Ion-Molecule Reactions," *Interactions between Ions and Molecules,* edited by P. Ausloos, *NATA Advanced Study Institute Series,* Plenum, New York, 1975, p. 185.

[41]Gislason, E.A., "Surface Crossing Model for Ion-Molecule Reactions," *Journal of Chemical Physics,* Vol. 57, 1972, p. 3396.

[42]Tully, J.C., "Trajectories in Ion-Molecule Reactions," *Berichte der Bunsengesellschaft fuer Physikalische Chemie,* Vol. 77, 1973, p. 557.

[43]Lindinger, W., Fehsenfeld, F.C., Schmeltekopf, A.L., and Ferguson, E.E., "Temperature Dependence of Some Ionospheric Ion-Neutral Reactions from 300-900 K," *Journal of Geophysical Research,* Vol. 79, 1974, p. 4753.

[44]McFarland, M., Albritton, D.L., Fehsenfeld, F.C., Schmeltekopf, A.L., and Ferguson, E.E., "Energy Dependence of the Rate Constant for the Relation $O^+ + NO \rightarrow NO^+ + O$," *Journal of Geophysical Research,* Vol. 79, 1974, p. 2005.

[45]Fehsenfeld, F.C., "The Reaction of O_2^+ with Atomic Nitrogen and NO^+, H_2O, and NO_2^+ with Atomic Oxygen," *Planetary and Space Science,* Vol. 25, 1977, p. 195.

[46]Ferguson, E.E., Bohme, D.K., Fehsenfeld, F.C., and Dunkin, D.B., "Temperature Dependence of Slow Ion-Atom Interchange Reactions," *Journal of Chemical Physics,* Vol. 50, 1969, p. 5038.

[47]Mul, P.M. and McGowan, J.W., "Merged Electron-Ion Beam Experiments III. Temperature Dependence of Dissociative Recombination for Atmospheric Ions NO^+, O_2^+, N_2^+," *Journal of Physics B: Atomic and Molecular Physics,* Vol. 12, 1979, p. 1591.

[48]"Potential Energy Curves for Dissociative Recombination," *Ion-Ion and Electron-Ion Collisions,* edited by S.L. Guberman, *NATO Advanced Study Institue Series,* Plenum, New York, 1982.

[49]Torr, M.R. and Torr, D.G., "Associative Ionization of $N(^2D)$ and O," *Planetary and Space Science,* Vol. 27, 1979, p. 1233.

[50]Baranger, M., "Spectral Line Broadening in Plasmas," *Atomic and Molecular Processes,* edited by D.R. Bates, Academic Press, New York, 1962.

[51]Wilson, K.H. and Nicolet, W.E., "Spectral Absorption Coefficients of Carbon, Nitrogen, and Oxygen Atoms," Lockheed, Palo Alto Research Lab., Palo Alto, Calif., Rept. 4-17-66-5, 1966.

[52]Anderson, P.W., "Pressure Broadening in the Microwave and Infrared Region," Physical Review, Vol. 76, 1949, p. 647.

[53]Tsao, C.J. and Curnutte, B., "Line Widths of Pressure-Broadened Spectral Lines," *Journal of Quantitative Spectroscopy & Radiative Transfer,* Vol. 2, 1962, p. 41.

[54]Benedict, W.S. and Kaplan, L.D., "Calculation of Line Widths in H_2O-N_2 Collisions," *Journal of Chemical Physics,* Vo. 30, 1959, p. 388.

[55]Benedict, W.S. and Kaplan, L.D., "Calculation of Line Widths in H_2O-H_2O and H_2O-O_2 Collisions," *Journal of Quantitative Spectroscopy & Radiative Transfer,* Vol. 4, 1964, p. 453.

[56]Varanasi, P., Tcowani, G.D., and Prasad, C.R., "Line Widths and Intensities in H_2O-CO_2 Mixtures," *Journal of Quantitative Spectroscopy & Radiative Transfer,* Vol. 11, 1971, p. 231.

[57]Tipping, R.H. and Herman, R.M., "Impact Theory for the Noble Gas Pressure-Induced HCl Vibration-Rotation and Pure Rotation Line Widths = 1," *Journal of Quantitative Spectroscopy & Radiative Transfer,* Vol. 10, 1970, p. 881.

[58]Herman, R.M. and Tipping, R.H., "Impact Theory for the Noble Gas Pressure-Induced HCl Vibration-Rotation and Pure Rotation Line Widths-II," *Journal of Quantitative Spectroscopy & Radiative Transfer,* Vol. 10, 1970, p. 897.

[59]Thomas, M.E. and Nordstrom, R.J., "The N_2-Broadened Water Vapor Absorption Line Shape and Infrared Continuum Absorption," *Journal of Quantitative Spectroscopy & Radiative Transfer,* Vol. 28, 1982, p. 81.